Monthly Notices
of the
ROYAL ASTRONOMICAL SOCIETY

MNRAS **452,** 2837–2844 (2015) doi:10.1093/mnras/stv1540

On the origin of the correlations between the accretion luminosity and emission line luminosities in pre-main-sequence stars

I. Mendigutía,[1]★ R. D. Oudmaijer,[1] E. Rigliaco,[2] J. R. Fairlamb,[1] N. Calvet,[3] J. Muzerolle,[4] N. Cunningham[1] and S. L. Lumsden[1]

[1]*School of Physics and Astronomy, University of Leeds, Woodhouse Lane, Leeds LS2 9JT, UK*
[2]*Swiss Federal Institute of Technology, Department of Physics-Institute for Astronomy, Wolfgang-Pauli-Strasse 27, CH-8093 Zurich, Switzerland*
[3]*Department of Astronomy, University of Michigan, 830 Dennison Building, 500 Church Street, Ann Arbor, MI 48109, USA*
[4]*Space Telescope Science Institute, 3700 San Martin Drive, Baltimore, MD 21218, USA*

Accepted 2015 July 8. Received 2015 July 6; in original form 2015 May 12

ABSTRACT

Correlations between the accretion luminosity and emission line luminosities ($L_{\rm acc}$ and $L_{\rm line}$) of pre-main-sequence (PMS) stars have been published for many different spectral lines, which are used to estimate accretion rates. Despite the origin of those correlations is unknown, this could be attributed to direct or indirect physical relations between the emission line formation and the accretion mechanism. This work shows that all (near-UV/optical/near-IR) $L_{\rm acc}$–$L_{\rm line}$ correlations are the result of the fact that the accretion luminosity and the stellar luminosity (L_*) are correlated, and are not necessarily related with the physical origin of the line. Synthetic and observational data are used to illustrate how the $L_{\rm acc}$–$L_{\rm line}$ correlations depend on the $L_{\rm acc}$–L_* relationship. We conclude that because PMS stars show the $L_{\rm acc}$–L_* correlation immediately implies that $L_{\rm acc}$ also correlates with the luminosity of all emission lines, for which the $L_{\rm acc}$–$L_{\rm line}$ correlations alone do not prove any physical connection with accretion but can only be used with practical purposes to roughly estimate accretion rates. When looking for correlations with possible physical meaning, we suggest that $L_{\rm acc}/L_*$ and $L_{\rm line}/L_*$ should be used instead of $L_{\rm acc}$ and $L_{\rm line}$. Finally, the finding that $L_{\rm acc}$ has a steeper dependence on L_* for T Tauri stars than for intermediate-mass Herbig Ae/Be stars is also discussed. That is explained from the magnetospheric accretion scenario and the different photospheric properties in the near-UV.

Key words: accretion, accretion discs – line: formation – methods: miscellaneous – stars: pre-main sequence – stars: variables: T Tauri, Herbig Ae/Be.

1 INTRODUCTION

The disc-to-star accretion rate is one of the most important parameters driving the evolution of pre-main-sequence (PMS) stars. However, it is difficult to directly measure the mass accretion rate, for which indirect empirical methods are necessary to estimate it. A widely used method exploits the fact that the accretion luminosity ($L_{\rm acc}$) correlates with the luminosity of various emission lines ($L_{\rm line}$). Despite the unknown origin of these correlations, they are being used to quickly estimate accretion rates. The $L_{\rm acc}$–$L_{\rm line}$ empirical correlations have been derived using samples of PMS stars by comparing their accretion luminosities, mostly obtained from the UV excess and line veiling, with the emission line luminosity (see e.g. Muzerolle, Hartmann & Calvet 1998b; Dahm 2008; Herczeg & Hillenbrand 2008; Fang et al. 2009; Rigliaco et al. 2012, and references therein). Currently, dozens of near-UV–optical–near-IR spectral lines have been found to correlate with $L_{\rm acc}$ for classical T Tauri (TT) stars (for instance, the hydrogen Balmer and Paschen series, He I, O I, Na ID and Ca II transitions, Br γ, etc; see e.g. Alcalá et al. 2014, hereafter AL14). The correlations of the accretion luminosity with several of these lines have been extended both to the sub-stellar and the intermediate-mass Herbig Ae/Be (HAeBe) regimes (Mohanty, Jayawardhana & Basri 2005; Donehew & Brittain 2011; Mendigutía et al. 2011, 2013; Rigliaco et al. 2011).

Apart from the observational effort involved to look for additional emission lines that could serve as accretion tracers, several investigations aim to provide physical links between some of the spectral transitions and the accretion process, which would explain the origin of the $L_{\rm acc}$–$L_{\rm line}$ correlations. In a nutshell, either the lines are directly tracing the accreting region (e.g. Muzerolle, Calvet & Hartmann 1998c; Muzerolle, Hartmann & Calvet 1998a; Kurosawa, Harries & Symington 2006; Rigliaco et al. 2015), or they trace the accretion indirectly, by probing the accretion-powered outflows and winds (e.g. Hartigan, Edwards & Ghandour 1995; Edwards et al. 2006; Kurosawa, Romanova & Harries 2011;

★ E-mail: I.Mendigutia@leeds.ac.uk

Kurosawa & Romanova 2012). The correlation with forbidden lines like [O I] (6300 Å) exhibited by HAeBes (Mendigutía et al. 2011) is more difficult to explain, as this line is not identified with accretion/winds but rather with the surface layers of the circumstellar discs (Acke, van den Ancker & Dullemond 2005). A further challenge to the various explanations of the origin of the $L_{\rm acc}$–$L_{\rm line}$ correlations is that the variations in the accretion rate as measured from the UV excess do not generally correlate with the observed changes in the line luminosities (Nguyen et al. 2009; Mendigutía et al. 2011, 2013; Costigan et al. 2012). However, time delays between different physical processes could be present (Dupree et al. 2012).

On the other hand, the accretion luminosity is also found to correlate with the luminosity of the central star (L_*). The $L_{\rm acc}$–L_* correlation extends over $\sim$ 10 orders of magnitude in $L_{\rm acc}$, and $\sim$ 7 orders of magnitude in L_*, covering all optically visible young stars from the sub-stellar to the HAeBe regime (see e.g. Clarke & Pringle 2006; Natta, Testi & Randich 2006; Tilling et al. 2008; Mendigutía et al. 2011; Fairlamb et al. 2015, and references therein). Based on a statistical analysis, Mendigutía et al. (2011) tentatively suggested that the correlation between the accretion luminosity and the luminosity of several emission lines in HAeBe stars could be driven by the common dependence of both luminosities on the stellar luminosity.

The main goal of this paper is to demonstrate the equivalence of the $L_{\rm acc}$–$L_{\rm line}$ and $L_{\rm acc}$–L_* correlations. In particular, we aim to show that all (near-UV, optical and near-IR) $L_{\rm acc}$–$L_{\rm line}$ correlations in PMS stars are driven by the relationship between the stellar luminosity and the accretion luminosity, and that therefore the accretion luminosity necessarily correlates with the luminosity of all spectral lines regardless of their physical origin. Section 2 introduces and partially re-analyses the $L_{\rm acc}$–L_* correlation in PMS stars. Section 3 shows the expression that links the $L_{\rm acc}$–L_* relationship with the $L_{\rm acc}$–$L_{\rm line}$ correlations. The inter-dependence between both types of correlations is illustrated in Section 4 using both synthetic data and observational data from the literature. Some implications from all the previous analysis are included in Section 5. Finally, Section 6 summarizes our main conclusions.

2 THE $L_{\rm acc}$–L_* CORRELATION

A representative example of the empirical correlation between the accretion and stellar luminosities[1] is shown in Fig. 1. It includes data from the literature for very low mass TTs and sub-stellar objects/companions ($\log(L_*/L_\odot) < -1.25$), TTs ($-1.25 < \log(L_*/L_\odot) < 0.75$), late-type HAeBes ($0.75 < \log(L_*/L_\odot) < 2.25$), and early-type HAeBes ($\log(L_*/L_\odot) > 2.25$). The sources belong to different star-forming regions. The graph shows that $L_{\rm acc}$ increases with L_*, with a relation steeper for the TTs than for the HAeBes.

According to Clarke & Pringle (2006) and Tilling et al. (2008), the upper bound of the $L_{\rm acc}$–L_* correlation ($L_{\rm acc} \sim L_*$) is the consequence of sample selection effects; the luminosity of most stars above that limit is dominated by accretion and these objects are in a younger, embedded phase without an optically visible photosphere. The lower bound ($L_{\rm acc} \sim 0.01 L_*$, mainly for objects with $L_* > L_\odot$) is limited by accretion detection thresholds (symbols with vertical bars in Fig. 1). The physical origin of the $L_{\rm acc}$–L_* correlation is the subject of active debate. This topic is not analysed here but we refer the reader to several related works (e.g. Padoan et al. 2005; Alexander & Armitage 2006; Dullemond, Natta & Testi 2006; Vorobyov & Basu 2008; Ercolano et al. 2014). Instead, our contribution below deals with the observed change in the slope of the $L_{\rm acc}$–L_* correlation between the TT and the HAeBe stars (Mendigutía et al. 2011; Fairlamb et al. 2015).

[1] Its counterpart, the relationship between mass accretion rate and stellar mass, can be derived from the $L_{\rm acc}$–L_* correlation using PMS tracks (see e.g. Clarke & Pringle 2006).

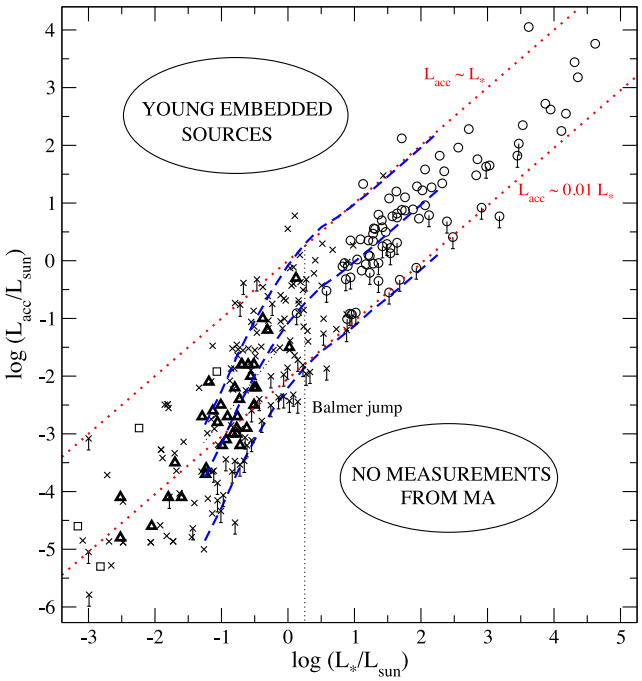

Figure 1. $L_{\rm acc}$–L_* correlation for sub-stellar objects and TTs in different star-forming regions (crosses; with vertical bars for upper limits; Natta et al. 2006; Herczeg & Hillenbrand 2008, and references therein), four (sub-) stellar/planetary companions around PMS stars (squares; Close et al. 2014; Zhou et al. 2014), the Lupus sample from AL14 (dark triangles) and HAeBes (circles; with vertical bars for upper limits; Mendigutía et al. 2011; Fairlamb et al. 2015). The red diagonal dotted lines indicate $L_{\rm acc} = L_*$ and $L_{\rm acc} = 0.01 L_*$. The three blue diagonal dashed lines represent the accretion luminosities expected from MA modelling for Balmer excesses of 0.70, 0.12 and 0.01 mag (top, mid and bottom lines, respectively). The vertical dotted line indicates the stellar luminosity at which the Balmer jump becomes apparent in the photospheric spectra (see also Fig. 2). [A colour version of this figure is available in the online journal.]

We constructed a sample of artificial stars representing the TT and HAeBe regime by using synthetic models of stellar atmospheres (Kurucz 1993). The properties of each object are provided in Table 1. Columns two and three show the stellar luminosity and effective temperature. From these, the stellar radii was derived, spanning between 0.7 and 4 $R_\odot$ (column 4). The stellar masses (column 5) were derived assuming $\log g = 4$, and cover the 0.2–6 $M_\odot$ range. Magnetospheric accretion (MA) shock modelling was carried out for each star by adding (blackbody) accretion contributions to the photospheric (Kurucz) spectra (see e.g. the reviews in Calvet, Hartmann & Strom 2000; Mendigutía 2013). Two representative examples are presented in Fig. 2 (left-hand panel). The shock model was applied following the usual recipes for both the TTs and HAeBes, and we refer the reader to Calvet & Gullbring (1998); Mendigutía et al. (2011) and Fairlamb et al. (2015) for further details. Three different values for the UV excess in the Balmer region of the spectra (from $\sim$3500 to 4000 Å, as defined in Mendigutía et al. 2013) were modelled for each object assuming typical values for

Table 1. Sample of artificial stars. Stellar parameters and accretion luminosities from MA. Columns two to five show the stellar luminosity (logarithmic scale, from the integrated Kurucz model atmospheres), effective temperature, stellar radius and mass. Columns six to eight show the MA accretion luminosities (logarithmic scale) corresponding to a minimum (m), typical (t) and maximum (M) Balmer excess of 0.01, 0.12 and 0.70 mag, respectively.

Star ♯	L_* [log $L_\odot$]	T_* (K)	R_* ($R_\odot$)	M_* ($M_\odot$)	$(L_{acc})_m$ [log $L_\odot$]	$(L_{acc})_t$ [log $L_\odot$]	$(L_{acc})_M$ [log $L_\odot$]
1	−1.25	3500	0.65	0.15	−4.85	−3.75	−2.84
2	−1.00	4000	0.66	0.16	−4.28	−3.17	−2.26
3	−0.75	4500	0.70	0.18	−3.64	−2.53	−1.61
4	−0.50	5000	0.75	0.20	−3.10	−1.99	−1.04
5	−0.25	5500	0.83	0.25	−2.62	−1.50	−0.53
6	0.00	6000	0.93	0.31	−2.20	−1.08	−0.08
7	0.25	6500	1.05	0.40	−1.85	−0.74	0.29
8	0.50	7000	1.21	0.53	−1.57	−0.45	0.58
9	0.75	7500	1.41	0.72	−1.36	−0.25	0.76
10	1.00	8000	1.65	0.99	−1.13	−0.02	0.98
11	1.25	8500	1.95	1.38	−0.89	0.22	1.21
12	1.50	9000	2.32	1.95	−0.64	0.47	1.46
13	1.75	9500	2.78	2.80	−0.40	0.72	1.71
14	2.00	10 000	3.34	4.05	−0.15	0.97	1.96
15	2.25	10 500	4.04	5.93	0.10	1.22	2.22

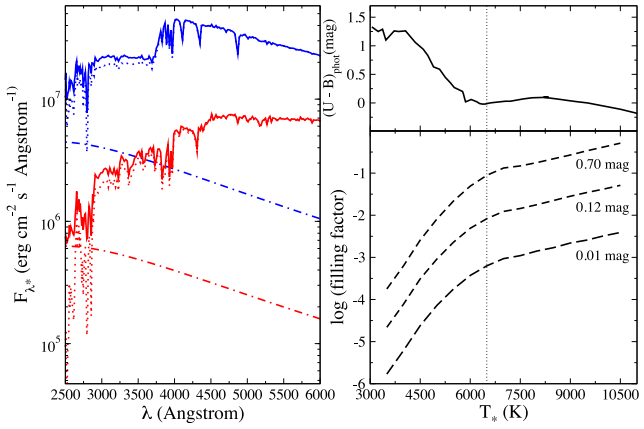

Figure 2. Left-hand panel: MA modelling of a typical Balmer excess (0.12 mag) for two representative stars with stellar temperatures of 7500 (blue) and 5500 *K* (red). The photospheric (Kurucz) spectra, the contribution from accretion and the total flux obtained from the combination of the previous are represented by the dotted, dot–dashed and solid lines, respectively. The fluxes are as they would be measured at the stellar surface. Right-hand panels: photospheric $U-B$ colours (taken from Kenyon & Hartmann 1995) characterizing the Balmer region of the spectrum (top) and filling factors necessary to reproduce a Balmer excess of 0.01, 0.12 and 0.70 mag (bottom) using MA, versus the stellar temperature. The vertical dotted line indicates the stellar temperature at which the Balmer jump becomes apparent in the photospheric spectra (see also Fig. 1). [A colour version of this figure is available in the online journal.]

the inward flux of energy carried by the accretion columns (10^{12} erg cm^2 s^{-1}) and the disc truncation radius ($5R_*$): a 'maximum' excess (0.70 mag), whose corresponding accretion contribution is $L_{acc} \sim L_*$ for $L_* \geq L_\odot$; a 'minimum' excess (0.01 mag) representative of the observational limit, and whose corresponding accretion contribution is $L_{acc} \sim 0.01 L_*$ for $L_* \geq L_\odot$; and finally, a 'typical' excess in-between the two previous (0.12 mag). The resulting accretion luminosities are shown in the last three columns of Table 1. These are plotted versus the corresponding L_* values (blue diagonal dashed lines in Fig. 1), matching the overall distribution of data. We note that excesses larger than 0.70 mag could still be measured for the less luminous sources ($L_* \leq L_\odot$) without reaching the upper bound ($L_{acc} \sim L_*$).

The fact that the accretion luminosity increases with the stellar luminosity is a natural consequence of MA shock modelling. This is illustrated in the left-hand panel of Fig. 2. When the same excess (flux ratio between the solid and dotted lines) is observed in stars of different stellar luminosity, the most luminous stars (blue dotted line) must necessarily have a larger accretion contribution (dot–dashed lines). In order to understand the different slope in the L_{acc}–L_* correlation for TT and HAeBe stars, it is important to recall that the accretion contribution, and therefore L_{acc}, is proportional to both the temperature of the accretion columns (T_{col}) and the filling factor (f), which represents the fraction of the stellar surface covered by the accretion shocks. Variations in T_{col} and f move the accretion-generated continuum excess along the wavelength axis and flux axis, respectively. The typical value for T_{col} is $\sim 10^4$ K across the TT and HAeBe regimes. Therefore, the excess peaks close to the Balmer region for both types of star. However, their photospheric spectra (i.e. when accretion is not present) are significantly different in that region. The Balmer jump becomes visible only for stars with log $(L_*/L_\odot) \geq 0.25$ (i.e. $T_* \geq 6500$ K).[2] This makes the spectra of stars with spectral types F and earlier more similar between them in the Balmer region than for later spectral types. Fig. 2 (top-right panel) illustrates the case; the photospheric U–B colour characterizing the Balmer region shows a steep dependence on the stellar temperature for cool stars, and flattens for hotter objects. Therefore, in order to reproduce a given Balmer excess, TTs require larger variations in the accretion luminosity than the ones that HAeBes need, for which the slope $\Delta L_{acc}/\Delta L_*$ decreases from the TT to the HAeBe regime. The accretion luminosity changes are mainly affected by variations in the filling factor. This is shown in Fig. 2 (bottom-right panel), where the filling factors that are needed to reproduce the minimum, typical and maximum model excesses are plotted against

[2] The Balmer jump disappears again in O stars with $T_* \geq 30\,000$ K.

the stellar temperature. The change of slope in this panel occurs at the temperature where the Balmer jump appears (∼6500 K), which corresponds to the stellar luminosity when the slope of the L_{acc}–L_* correlation changes (log ($L_*/L_\odot$) ∼ 0.25). It is noted that we have applied basic MA modelling without considering aspects like the chromospheric contribution to the spectra of TT stars (Manara et al. 2013) or changes in the disc truncation radius depending on the stellar mass regime (Muzerolle et al. 2004; Mendigutía et al. 2011; Cauley & Johns-Krull 2014). These factors could change the accretion estimates by less than 0.5 dex, without significantly affecting the modelled results in Figs 1 and 2.

In summary, the observed difference in the L_{acc}–L_* correlation between TTs and HAeBes can be explained from the MA scenario and the differences in the near-UV stellar properties between both types of stars. However, we emphasize that the overall L_{acc}–L_* correlation is not a mere consequence of the MA shock modelling but most probably reflects a deeper physical relationship between both parameters (see e.g. the references at the beginning of this section). For example, the specific slopes shown by different samples in different environments (see e.g the Lupus sample with solid triangles in Fig. 1) cannot simply be explained from MA. Moreover, the L_{acc}–L_* correlation seems to arise also in embedded, younger sources, when the accretion luminosities are estimated from a variety of methods (Beltrán & de Wit, in preparation). Regardless of the underlying physical origin of the L_{acc}–L_* correlation, for the rest of the paper it will be enough to remind that this arises whenever a significant sample of PMS stars is considered.

3 THE ACCRETION–STELLAR-LINE LUMINOSITY RELATION

The relation between the accretion and stellar luminosities is usually expressed in the literature as $L_{acc} \propto L_*^b$. This can also be written as a linear expression, which is a reasonable approach when the TT and HAeBe regimes are studied separately. For a given star, we will assume that L_{acc} and L_* can then be related by

$$\log\left(\frac{L_{acc}}{L_\odot}\right) = a + b \times \log\left(\frac{L_*}{L_\odot}\right), \quad (1)$$

with a and b constants that depend on the star considered. When a sample of stars is studied, a and b represent the intercept and the slope of a linear fit to the data. This situation will be analysed in Section 4.

The luminosity of a spectral line can be computed by multiplying the line equivalent width (EW) and the luminosity (per unit wavelength) of the adjacent continuum (L_λ^c):

$$L_{line} = L_\lambda^c \times EW = \left(\frac{\alpha \cdot EW}{\beta}\right) \times L_*, \quad (2)$$

with α the (dimensionless) excess of the (dereddened) continuum with respect to the photosphere at the wavelength of the line ($\alpha = L_\lambda^c/L_{\lambda *} \geqq 1$), and β the ratio between the total stellar luminosity and the stellar luminosity at that wavelength ($\beta = L_*/L_{\lambda *} \gg 1$, in units of wavelength). The stellar luminosity in the second term of equation (2) was introduced in equation (1), obtaining

$$\log\left(\frac{L_{acc}}{L_\odot}\right) = A + B \times \log\left(\frac{L_{line}}{L_\odot}\right), \quad (3)$$

which is again a linear expression, with

$$A = a - b \times \log\left(\frac{L_{line}}{L_*}\right),$$
$$B = b, \quad (4)$$

Table 2. Sample of artificial stars. Continuum and line properties. Columns two to five list the luminosity of the continuum at 6000 Å (logarithmic scale), the ratio between the total, star + accretion, luminosity and the stellar luminosity at 6000 Å, a random EW of an hypothetical emission line assigned to each star (between 1 and 10 Å), and its corresponding luminosity at 6000 Å (logarithmic scale).

Star ♯	L^c_{6000} [log $L_\odot$ Å]	$\beta(\lambda = 6000$ Å)	EW (Å)	L_{6000} [log $L_\odot$]
1	−5.64	24 317	7	−4.79
2	−5.13	13 363	5	−4.43
3	−4.74	9790	2	−4.44
4	−4.42	8343	9	−3.47
5	−4.14	7792	1	−4.14
6	−3.88	7573	2	−3.58
7	−3.63	7587	4	−3.03
8	−3.39	7698	7	−2.54
9	−3.15	7880	10	−2.15
10	−2.92	8284	3	−2.44
11	−2.69	8773	6	−1.91
12	−2.48	9603	8	−1.58
13	−2.27	10 581	4	−1.67
14	−2.07	11 723	1	−2.07
15	−1.86	12 905	6	−1.08

where $L_{line}/L_* = \alpha EW/\beta$, is the line to stellar luminosity ratio. Therefore, if the accretion luminosity of a given star can be derived from its stellar luminosity through equation (1), then the same accretion luminosity can be recovered from the luminosity of any emission line through equations (3) and (4), with A and B constants that depend on the star and the line considered. Equations (1) and (3) are equivalent because both express a common dependence of the accretion luminosity on the stellar luminosity (equation 2).

4 THE DEPENDENCE OF THE L_{acc}–L_{line} CORRELATIONS ON THE L_{acc}–L_* RELATION

In this section, we use both synthetic and empirical data to illustrate the dependence of the L_{acc}–L_{line} correlations on the L_{acc}–L_* relation. Our first analysis provides a simple qualitative example on how the shape of the L_{acc}–L_* relationship has a strong effect on the L_{acc}–L_{line} correlations. We use the sample of artificial stars introduced in the previous section (see the first five columns of Table 1). The Kurucz models were used to calculate L_λ^c and β at 6000 Å, whose values are presented in columns two and three of Table 2. Random EWs (between 1 and 10 Å, column four) are assigned to each object. These range in EW is representative of emission lines with intermediate strength such as the Ca II or O I transitions. The luminosity of an artificial emission line at 6000 Å (column five) can then be obtained from equations (2).

The top-left panel of Fig. 3 shows two different L_{acc}–L_* linear relations assumed for the sample. Both have the same intercept but a different slope. The reverse is shown in the bottom-left panel, in which the slope is kept constant and the intercept varies. The right-hand panels show the corresponding accretion luminosities versus the luminosity of the artificial line at 6000 Å. The L_{acc}–L_{line} correlations follow the changes introduced in the $L_{acc} - L_*$ relation, varying their slopes and intercepts. The range in the EW used only affects the scatter of the L_{acc}–L_{line} correlation, but this is ultimately determined by the $L_{acc} - L_*$ relation. As introduced in Section 3,

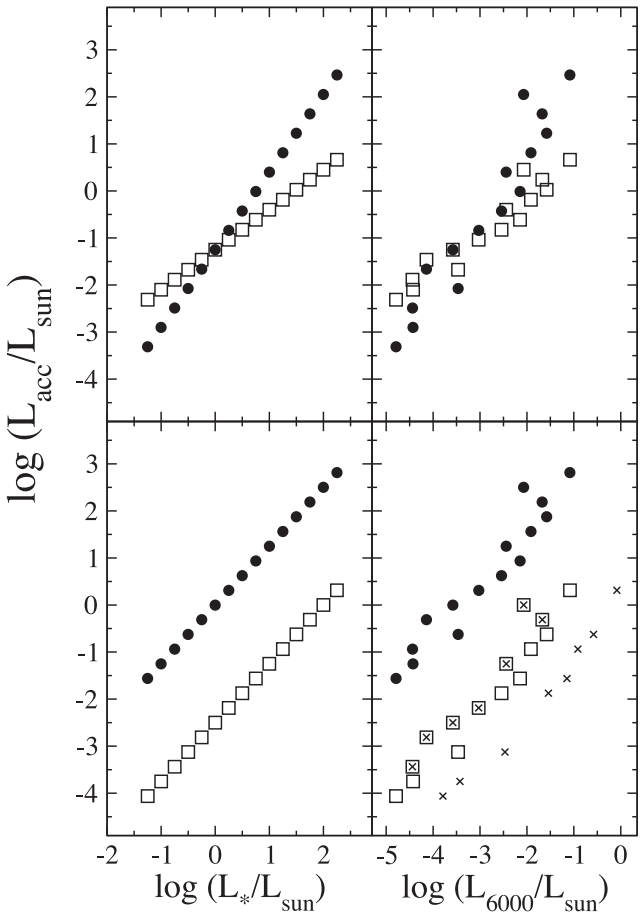

Figure 3. Results for the sample of artificial stars, showing how changes in the assumed L_{acc}–L_* correlation (left-hand panels) have an effect on the L_{acc}–L_{line} relation (right-hand panels) by changing the slope (top panels) and the intercept (bottom panels) of the former correlations. The crosses in the bottom-right panel represent the line luminosities obtained from a wider EW range, when the EWs ≥ 5 Å in column 5 of Table 2 are multiplied by a factor 10.

the contribution of the continuum to the line luminosity dominates over the EW, and both the continuum and the accretion luminosities are correlated with the stellar luminosity. In order to illustrate this, the EW range was increased multiplying by 10 all the EWs ≥ 5 Å in column 4 of Table 2, and keeping the rest unmodified. This range in EW is representative of a strong emission line such as H α. The new line luminosities are plotted with crosses in the bottom-right panel of Fig. 3, showing that for wider (narrower) EW ranges, the scatter in the L_{acc}–L_{line} correlation increases (decreases), but the correlation remains.

Before using real data from the literature to illustrate how the L_{acc}–L_{line} empirical correlations are driven by the L_{acc}–L_* relation, the equations described in the previous section have to be slightly modified. There, the values of L_{acc} were given by equations (1) and (3), where a, b, A and B differ depending on the individual star and spectral line. In practice, the values for the slopes and intercepts of these equations are estimated using linear regression fitting, which provide unique a and b values for a given sample of stars, as well as unique A and B values for a given spectral line. In this case it can be shown (see Appendix A) that the slopes and intercepts of the L_{acc}–L_* and the L_{acc}–L_{line} empirical correlations are related by

$$A \sim a - b \times \epsilon \times \left\langle \log \frac{L_{line}}{L_*} \right\rangle ;$$
$$B = b \times \epsilon;$$
$$\epsilon = \frac{r_{line} \times \sigma_*}{r_* \times \sigma_{line}} \sim 1, \quad (5)$$

where A, a; B, and b represent the intercepts and slopes of the L_{acc}–L_* and L_{acc}–L_{line} correlations, as derived from least-squares linear regression fitting, $\langle \log L_{line}/L_* \rangle$ the mean (logarithmic) line to stellar luminosity ratio, r_* and r_{line} the correlation coefficients of the L_{acc}–L_* and L_{acc}–L_{line} linear fits, and σ_* and σ_{line} the standard deviations of the log $(L_*/L_\odot)$ and log $(L_{line}/L_\odot)$ values.

In short, when the empirical L_{acc}–L_* and L_{acc}–L_{line} correlations are compared, equations (5) should be used instead of equations (4). These are slightly modified by including the ϵ parameter, which accounts for the fact that the empirical correlations are in practice derived from (least-squares) linear fitting.[3]

We use the observational data in AL14 to illustrate the dependence of the L_{acc}–L_{line} empirical correlations on the $L_{acc} - L_*$ relation. These authors studied a sample of 36 low-mass TTs in the Lupus star-forming region, for which they derived stellar parameters, accretion rates from the UV excess, and L_{acc}–L_{line} empirical correlations for dozens of emission lines in the spectral range from the near-UV to the near-infrared. To our knowledge, this work contains the largest number of spectral lines for which this type of correlations are derived. Another advantage is that for each star the accretion luminosity and the luminosity of all spectral lines were derived from the same spectrum, avoiding the problem of variability. In addition, all the stars are located at a similar distance, which guarantees that the correlations were not artificially stretched when the fluxes are multiplied by the squared distances to derive the (accretion and line) luminosities. Therefore, we consider the $L_{acc} - L_*$ and L_{acc}–L_{line} correlations in AL14 as representative for similar correlations provided in the literature (see e.g the references in Section 1).

The top panel of Fig. 4 shows the accretion and stellar luminosities of the stars studied by AL14. The observed trend is best fitted by log $(L_{acc}/L_\odot) \sim -1.3 + 1.4 \times$ log $(L_*/L_\odot)$ (solid line). The slopes and intercepts of the L_{acc}–L_{line} empirical correlations derived by AL14 (see their table 4), which are exactly recovered by equations (5), are plotted in the mid and bottom panels of Fig. 4 versus ϵ and $\epsilon \times \langle \log L_{line}/L_* \rangle$, respectively. The mid panel shows that the slopes of the L_{acc}–L_{line} empirical correlations are a factor ϵ smaller than the slope of the L_{acc}–L_* correlation shown by the sample. As expected from equations (5), the L_{acc}–L_{line} empirical correlations become steeper when ϵ increases, eventually reaching a slope of $\sim$1.4 for $\epsilon = 1$. The bottom panel shows the expected linear decrease of the intercepts of the L_{acc}–L_{line} correlations with the (ϵ-modified) line to stellar luminosity ratio. Equations (5) also imply that the typical (mean) slope of all L_{acc}–L_{line} correlations is given by the slope of the $L_{acc} - L_*$ correlation of the sample, corrected by the mean value of ϵ; $\langle B \rangle = b \times \langle \epsilon \rangle$. Similarly, it can be derived that the mean intercept of the L_{acc}–L_{line} correlations is given by $\langle A \rangle = a - b \times \langle \epsilon \times \langle \log L_{line}/L_* \rangle \rangle$. The two previous relations are also observed in the AL14 data, the mean values indicated with

[3] Linear regression fits obtained from methods different than the usual least-squares are not considered in this work. The ϵ parameter should be eventually modified if other linear regression methods are used.

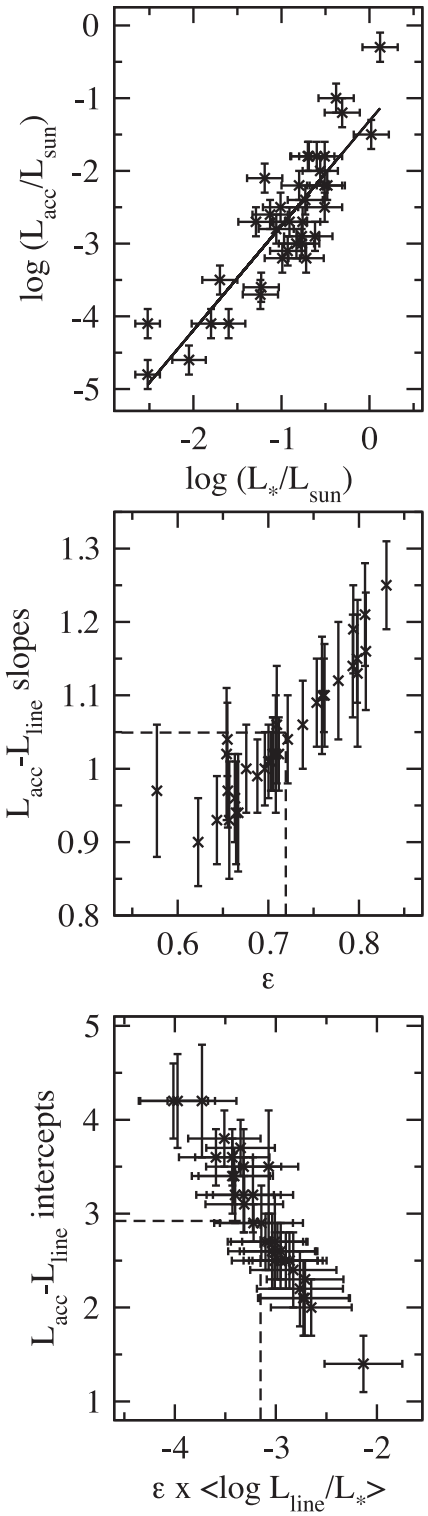

Figure 4. Based on results in AL14. Top panel: accretion versus stellar luminosity. The best linear fit is $\log(L_{\rm acc}/L_{\odot}) \sim -1.3 + 1.4\times\log(L_{*}/L_{\odot})$ (solid line). Mid and bottom panels: slopes and intercepts of the $L_{\rm acc}$–$L_{\rm line}$ empirical correlations versus the ϵ parameter (mid-panel) and the ϵ-modified mean (logarithmic) line to stellar luminosity ratio (bottom panel). The dashed lines indicate the mean values for the x and y axis, related from the slope and intercept of the top panel correlation by: $\langle y\rangle = 1.4\langle x\rangle$ (mid panel), and $\langle y\rangle = -1.3$–$1.4\langle x\rangle$ (bottom panel).

the dashed lines perpendicular to both axis in the mid and bottom panels of Fig 5.

In summary, the analysis of both a sample of artificial stars and representative empirical data shows that the $L_{\rm acc}$–$L_{\rm line}$ correlations are driven by the underlying $L_{\rm acc} - L_{*}$ relation shown by the sample of stars under study.

5 CONSEQUENCES

The first consequence of the analysis in the previous sections is that the fact that PMS stars show the $L_{\rm acc} - L_{*}$ correlation immediately implies that $L_{\rm acc}$ also correlates with the luminosity of any (near-UV–optical–near-IR) emission line, regardless of the physical origin of the spectral transition. Indeed, it even correlates with the luminosity of a randomly general artificial emission line (right-hand panels of Fig. 3). As mentioned earlier, the scatter of the $L_{\rm acc}$–$L_{\rm line}$ correlations increases when the lines' EWs exhibit a larger range. A similar effect occurs for stars with strong excess at short, UV, wavelengths and long, IR, wavelengths. For lines observed at these short and long wavelengths, the ratio $\alpha{\rm EW}/\beta$ (i.e. the line to stellar luminosity ratio; equation 2) becomes significant, which could make the $L_{\rm acc}$–$L_{\rm line}$ correlations much more scattered or eventually disappear.

For the other lines, the $L_{\rm acc}$–$L_{\rm line}$ correlations are mainly determined by the $L_{\rm acc} - L_{*}$ dependence shown by the sample under analysis. The intercepts and slopes provided in the literature for the $L_{\rm acc} - L_{*}$ correlation (a and b in equation 1) vary depending on the sample of stars considered (Fairlamb et al. 2015, and references therein). Based on those works, a conservative observational limit is $-2.5 \leq a \leq 0$, $0.8 \leq b \leq 2$. Consequently (see equations 4 and 5), the slopes of all $L_{\rm acc}$–$L_{\rm line}$ empirical correlations should also range in between ~ 0.8 and 2, whereas the intercepts should all be > 0 and decrease as the mean line to stellar luminosity ratio increases. These predictions agree with all $L_{\rm acc}$–$L_{\rm line}$ published correlations based on observational data, to our knowledge. Interestingly, if two samples of stars show a different slope in their corresponding $L_{\rm acc}$–L_{*} correlations, then the slopes of the $L_{\rm acc}$–$L_{\rm line}$ ones are simply related via $B' \sim B \times (b'/b)$ (assuming that the ϵ factors in equation (5) are roughly similar in both samples). This effect has already been observed. Mendigutía et al. (2011) reported a slight decrease in the slope of the $L_{\rm acc}$–L_{*} correlation of a sample of 34 HAeBe stars with respect to TTs (see also Fig. 1 and Fairlamb et al. 2015). As discussed there, the slopes of the $L_{\rm acc}$–$L_{\rm line}$ empirical correlations for the three lines studied (H α, [O I] (6300 Å), and Br γ) also show a similar decrease.

That $L_{\rm acc}$ correlates with $L_{\rm line}$ is ultimately due to a common dependence of both luminosities on the stellar brightness. Because of this and the reasons above, the $L_{\rm acc}$–$L_{\rm line}$ correlations alone cannot be seen as proof for either a direct or indirect physical connection between the spectral transitions and the accretion process. However, they are still useful expressions that can be applied to easily derive accretion luminosities without the need for sophisticated modelling of the UV excess. A basic measurement of a line luminosity suffices. Given that both observational $L_{\rm acc}$–$L_{\rm line}$ and $L_{\rm acc}$–L_{*} correlations show a roughly similar scatter (around $\pm$ 1 dex in $L_{\rm acc}$), the latter can also be used to easily derive accretion rates from the stellar luminosity.

Analogously, since $L_{\rm line}$ necessarily correlates with L_{*} (equation 2), correlations between $L_{\rm line}$ and L_{*} alone cannot be taken as a possible physical link between the spectral transition and the stellar luminosity (see also Natta et al. 2014). By extension, the luminosities of two different emission lines should also correlate with each

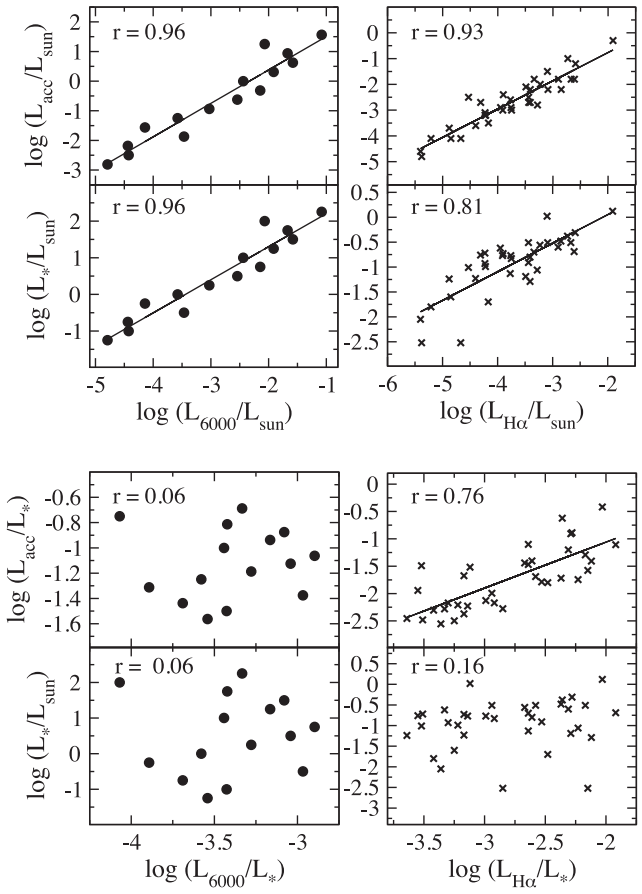

Figure 5. Comparison between different luminosities normalized by the solar and the stellar luminosity, as indicated in the axes' labels. The left-hand panels refer to the sample of artificial stars in Table 2, and the right-hand panels to real observations from AL14. Linear regression fits are overplotted for those cases with large enough correlation coefficients ($r > 0.50$; r-values indicated in each panel).

other because of the common dependence on the stellar luminosity. Again, exceptions are possible for lines at short/long wavelengths in stars with strong excesses (see e.g. Meeus et al. 2012).

In order to infer from correlations possible physical links involving the luminosity of a spectral line or the accretion luminosity, it is necessary to get rid of the common dependence of both parameters on the stellar luminosity. This can be done by dividing L_{line} and L_{acc} by L_*. Fig. 5 (top panels) shows the L_{acc}–L_{line} correlation for the sample of artificial stars from Table 2 and a given $L_{acc} - L_*$ relation, and the intrinsic correlation between the stellar and line luminosities. However, the bottom-left panels show that both L_{acc}/L_* and L_* do not correlate with L_{line}/L_*, as expected from an artificial line created with random EWs. The right-hand panels of the same figure show the results of the same exercise using real data from AL14. As expected, the H α luminosity correlates with both the accretion and stellar luminosities, which as we have discussed has no possible physical interpretation. In contrast with the previous example, in this case the Hα line to stellar luminosity ratio is still correlated with the accretion to stellar luminosity ratio but not with the stellar luminosity itself, supporting the idea that this line is mainly driven by accretion and not by the stellar brightness.

With this perspective in mind, we have confirmed that all line luminosities provided in AL14 correlate with each other, as expected. We also have checked that when the line luminosities are normalized by the stellar luminosities, some correlations remain while others disappear, indicating the presence or absence of a physical link between the different spectral transitions. For example, for Hα and Br γ the correlation is not only between their line luminosities but also between their line to stellar luminosity ratios, suggesting a common physical origin for both transitions. In contrast, despite the fact that the luminosities of the He II (4686 Å) and the Ca II (8498 Å) lines correlate, their line to stellar luminosities do not show a significant correlation, suggesting a different physical origin.

Finally, when the general $L_{acc} - L_*$ correlation analysed in Section 2 is transformed into L_{acc}/L_* versus L_*, no trend is shown either for the whole sample or for specific samples like the Lupus objects in AL14. The vast majority of the objects have $0.01 \leq L_{acc}/L_* \leq 1$ (diagonal dotted lines in Fig. 1) for all stellar luminosity bins. The typical value of L_{acc}/L_* is 0.1, which corresponds to the modelled, typical Balmer excess of 0.12 mag. For the less luminous sources ($L_* < L_\odot$), smaller L_{acc}/L_* ratios can still be obtained from the same Balmer excess detection limit. As discussed in Section 2, this is the expected consequence of the MA scenario and the photospheric properties of the stars in the near-UV.

It is beyond the scope of this work to carry out a detailed study on physical correlations involving stellar, line and accretion luminosities. Instead, we have provided several examples to suggest that correlation analysis aiming to infer physical consequences should use L_{line}/L_* and L_{acc}/L_* and not simply L_{line} and L_{acc}.

6 SUMMARY AND CONCLUSIONS

The $L_{acc} - L_*$ empirical correlation in PMS stars has been partially re-analysed taking into account the newly available accretion rates for HAeBes. Despite the physical origin of the $L_{acc} - L_*$ correlation remains subject to debate, the observed change of slope from the TT to the HAeBe regime can be understood from the MA scenario and the near-UV photospheric properties of the stars.

We have shown that the fact that PMS stars show the $L_{acc} - L_*$ correlation immediately implies that L_{acc} also correlates with the luminosity of any (near-UV, optical, near-IR) emission line, regardless of the physical origin of the spectral transition. The overall L_{acc}–L_{line} trends are mainly governed by the L_{acc}–L_* correlation shown by the sample of stars under analysis. In particular, the slopes of the L_{acc}–L_{line} empirical correlations should typically be between ~0.8 and 2 for all spectral lines, which are the observational limits for the slope of the L_{acc}–L_* relation. The intercepts also depend on the L_{acc}–L_* correlation, all of which are > 0 and increasing as the line to stellar luminosity ratio decreases.

Despite the fact that the L_{acc}–L_{line} correlations alone do not constitute an indication of any direct or indirect physical link between the spectral transitions and accretion, they are a useful tool to easily derive estimates of the accretion rates. The $L_{acc} - L_*$ correlations can be used for the same purpose. Similarly, correlations between stellar and line luminosities, or between different line luminosities, do not indicate a physical relation between the parameters involved. Instead, we suggest that the line to stellar and accretion to stellar luminosity ratios should be used when investigating the possible physical origin of the various correlations.

ACKNOWLEDGEMENTS

The authors sincerely acknowledge A. Natta, W.J. de Wit and M. Beltrán for the fruitful discussions that have served to improve the

contents of this manuscript, as well as the anonymous referee for her/his useful comments.

REFERENCES

Acke B., van den Ancker M. E., Dullemond C. P., 2005, A&A, 436, 209
Alcalá J. M. et al., 2014, A&A, 561, A2 (AL14)
Alexander R. D., Armitage P. J., 2006, ApJ, 639, L83
Calvet N., Gullbring E., 1998, ApJ, 509, 802
Calvet N., Hartmann L., Strom S. E., 2000, in Mannings V., Boss A. P., Russell S. S., eds, Protostars and Planets IV. Univ. Arizona Press, Tucson, AZ, p. 377
Cauley P. W., Johns-Krull C. M., 2014, ApJ, 797, 112
Clarke C. J., Pringle J. E., 2006, MNRAS, 370, L10
Close L. M. et al., 2014, ApJ, 781, L30
Costigan G., Scholz A., Stelzer B., Ray T., Vink J. S., Mohanty S., 2012, MNRAS, 427, 1344
Dahm S. E., 2008, AJ, 136, 547
Donehew B., Brittain S., 2011, AJ, 141, 46
Dullemond C. D., Natta A., Testi L., 2006, ApJ, 645, L69
Dupree A. K. et al., 2012, ApJ, 750, 73
Edwards S., Fischer W., Hillenbrand L., Kwan J., 2006, ApJ, 646, 319
Ercolano B., Mayr D., Owen J. E., Rosotti G., Manara C. F., 2014, MNRAS, 439, 256
Fairlamb J. R., Oudmaijer R. D., Mendigutía I., Ilee J. D., van den Ancker M. E., 2015, MNRAS, in press
Fang M., van Boekel R., Wang W., Carmona A., Sicilia-Aguilar A., Henning Th., 2009, A&A, 504, 461
Hartigan P., Edwards S., Ghandour L., 1995, ApJ, 452, 736
Herczeg G. J., Hillenbrand L. A., 2008, ApJ, 681, 594
Kenyon S. J., Hartmann L., 1995, ApJS, 101, 117
Kurosawa R., Romanova M. M., 2012, MNRAS, 426, 2901
Kurosawa R., Harries T. J., Symington N. H., 2006, MNRAS, 370, 580
Kurosawa R., Romanova M. M., Harries T. J., 2011, MNRAS, 416, 2623
Kurucz R. L., 1993, SYNTHE Spectrum Synthesis Programs and Line Data, Kurucz CD-ROM 18. Smithsonian Astrophysical Observatory, Cambridge, MA
Manara C. F. et al., 2013, A&A, 551, A107
Meeus G. et al., 2012, A&A, 544, A78
Mendigutía I., 2013, Astron. Nachr., 334, 129
Mendigutía I., Calvet N., Montesinos B., Mora A., Muzerolle J., Eiroa C., Oudmaijer R. D., Mern B., 2011, A&A, 535, A99
Mendigutía I. et al., 2013, ApJ, 776, 44
Mohanty S., Jayawardhana R., Basri G., 2005, ApJ, 626, 498
Muzerolle J., Hartmann L., Calvet N., 1998a, AJ, 116, 455
Muzerolle J., Hartmann L., Calvet N., 1998b, AJ, 116, 2965
Muzerolle J., Calvet N., Hartmann L., 1998c, ApJ, 492, 743
Muzerolle J., D'Alessio P., Calvet N., Hartmann L., 2004, ApJ, 617, 406
Natta A., Testi L., Randich S., 2006, A&A, 452, 245
Natta A., Testi L., Alcalá J. M., Rigliaco E., Covino E., Stelzer B., D'Elia V., 2014, A&A, 569, A5
Nguyen D. C., Scholz A., van Kerkwijk M. H., Jayawardhana R., Brandeker A., 2009, ApJ, 694, L153
Padoan P., Kritsuk A., Norman M., Nordlund Å., 2005, ApJ, 622, L61
Rigliaco E., Natta A., Randich S., Testi L., Covino E., Herczeg G., Alcal J. M., 2011, A&A, 526, L6
Rigliaco E., Natta A., Testi L., Randich S., Alcal J. M., Covino E., Stelzer B., 2012, A&A, 548, A56
Rigliaco E. et al., 2015, ApJ, 801, 31
Tilling I., Clarke C. J., Pringle J. E., Tout C. A., 2008, MNRAS, 385, 1530
Vorobyov E. I., Basu S., 2008, ApJ, 676, L139
Zhou Y., Herczeg1 G. J., Kraus A. L., Metchev S., Cruz K. L., 2014, ApJ, 783, L1

APPENDIX A: RELATION BETWEEN THE $L_{\rm acc}$–$L_{\rm line}$ AND $L_{\rm acc}$–L_* LINEAR REGRESSION CORRELATIONS

Consider a sample of N stars for which measurements of accretion and stellar luminosities [log $(L_{\rm acc}/{\rm L}_\odot)_1$,..., log $(L_{\rm acc}/{\rm L}_\odot)_N$; log $(L_*/{\rm L}_\odot)_1$,..., log $(L_*/{\rm L}_\odot)_N$)] are available. A linear fit to the data provides an expression that links both variables through

$$\log\left(\frac{L_{\rm acc}}{{\rm L}_\odot}\right) = a + b \times \log\left(\frac{L_*}{{\rm L}_\odot}\right), \tag{A1}$$

with a and b constants representing the intercept and the slope, which from least-squares linear regression are given by

$$b = r_* \times \left(\frac{\sigma_{\rm acc}}{\sigma_*}\right);$$
$$a = \left\langle \log\left(\frac{L_{\rm acc}}{{\rm L}_\odot}\right)\right\rangle - b \times \left\langle \log\left(\frac{L_*}{{\rm L}_\odot}\right)\right\rangle, \tag{A2}$$

where r_* is the correlation coefficient (~ 1 for well correlated data), and $\sigma_{\rm acc}$, σ_*; $\langle \log L_{\rm acc}/{\rm L}_\odot\rangle$, and $\langle \log L_*/{\rm L}_\odot\rangle$ the standard deviations and the means of the log $(L_{\rm acc}/{\rm L}_\odot)_i$ and log $(L_*/{\rm L}_\odot)_i$ values, respectively.

Similarly, if for the same sample of stars there are additional measurements of the luminosity of a given emission line [log $(L_{\rm line}/{\rm L}_\odot)_1$,..., log $(L_{\rm line}/{\rm L}_\odot)_N$], then a linear fit provides

$$\log\left(\frac{L_{\rm acc}}{{\rm L}_\odot}\right) = A + B \times \log\left(\frac{L_{\rm line}}{{\rm L}_\odot}\right), \tag{A3}$$

with A and B constants given by least-squares linear regression

$$B = r_{\rm line} \times \left(\frac{\sigma_{\rm acc}}{\sigma_{\rm line}}\right);$$
$$A = \left\langle \log\left(\frac{L_{\rm acc}}{{\rm L}_\odot}\right)\right\rangle - B \times \left\langle \log\left(\frac{L_{\rm line}}{{\rm L}_\odot}\right)\right\rangle, \tag{A4}$$

where the correlation coefficient, standard deviations, and means now refer to the [log $(L_{\rm acc}/{\rm L}_\odot)_i$, log $(L_{\rm line}/{\rm L}_\odot)_i$] values.

The standard deviation $\sigma_{\rm acc}$ can be found in the expression for b of equation (A2), and then introduced in the expression for B of equation (A4), providing the expression relating the slopes of the $L_{\rm acc}$–L_* and $L_{\rm acc}$–$L_{\rm line}$ linear correlations:

$$B = \epsilon \times b;$$
$$\epsilon = \frac{r_{\rm line} \times \sigma_*}{r_* \times \sigma_{\rm line}}. \tag{A5}$$

On the other hand, the mean value $\langle \log L_{\rm acc}/{\rm L}_\odot\rangle$ can be found in the expression for a of equation (A2), and introduced in the expression for A of equation (A4). Also considering equation (A5), the expression that relates both intercepts is

$$A = a - b \times \epsilon \times \left[\left\langle \log\left(\frac{L_{\rm line}}{L_*}\right)\right\rangle - \left(\frac{1-\epsilon}{\epsilon}\right) \times \left\langle \log\left(\frac{L_*}{{\rm L}_\odot}\right)\right\rangle\right]. \tag{A6}$$

The third term could been neglected ($(1-\epsilon)/\epsilon \sim 0$) compared with the two other terms in the previous equation.

This paper has been typeset from a TEX/LATEX file prepared by the author.